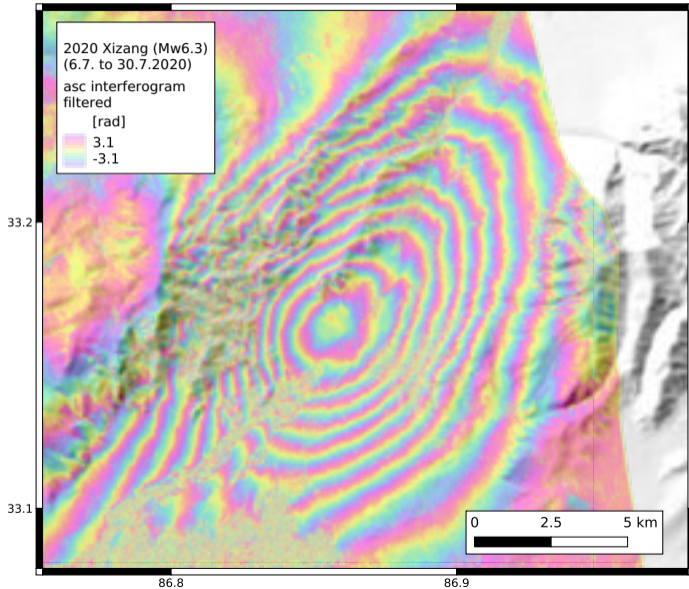


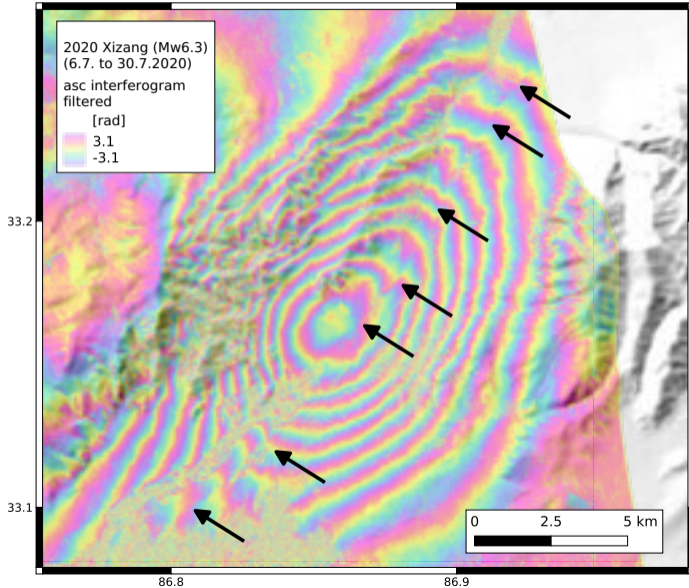
Locus and type of synseismic, secondary fault slip during large-magnitude earthquakes

Henriette Sudhaus, John Begg, Vasiliki Mouslopoulou, Tilman May

henriette.sudhaus@ifg.uni-kiel.de
www.bridges.uni-kiel.de



A Mw6.3 in Xizang, Tibet, 2020
ascending S1 interferogram



A Mw6.3 in Xizang, Tibet, 2020

ascending S1 interferogram

“**synseismic**”: likely happens **during** the earthquake,
is observed in coseismic interferograms

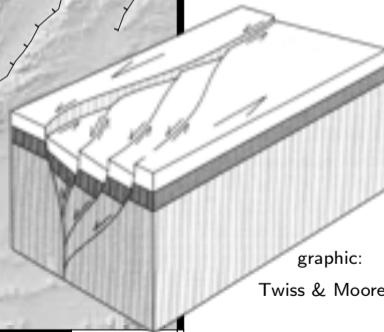
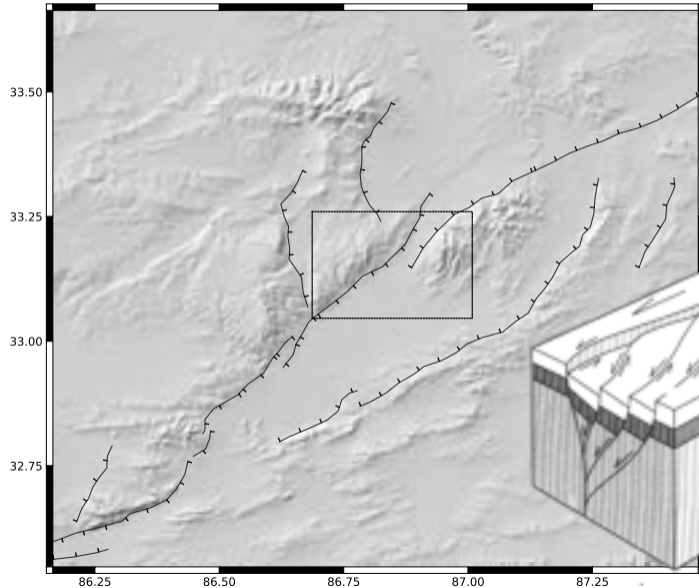
“**secondary**”: on a lower order of amplitude compared to main rupture deformation

“**fault slip**“: activation/movement along faults

arrows point to phase steps

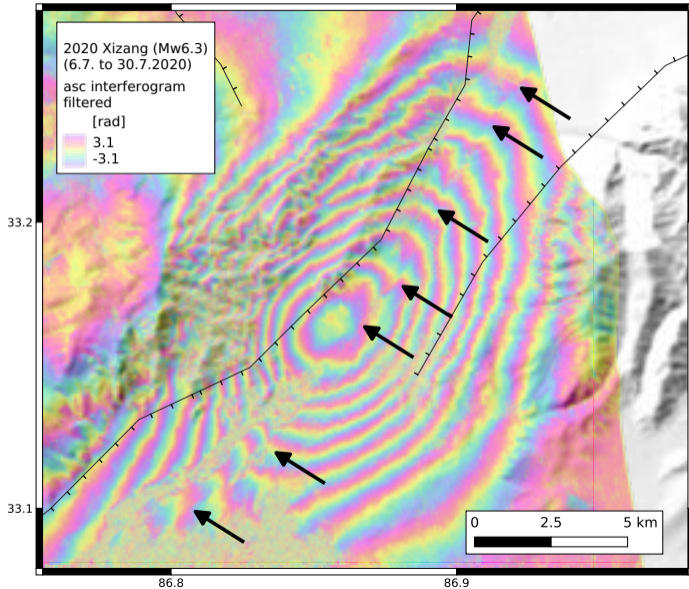
A Mw6.3 in Xizang, Tibet, 2020

Quick glimpse at regional tectonics
Faults based on the database
"Active Faults of Eurasia"



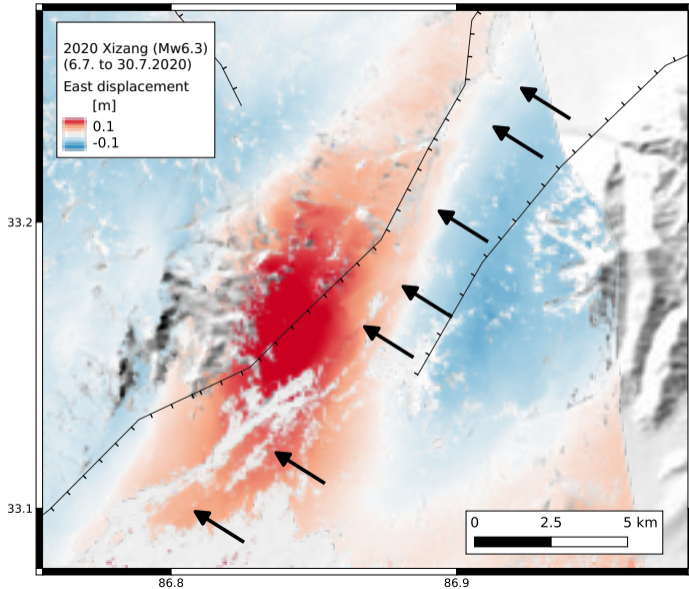
negative
flower structure

graphic:
Twiss & Moores (1992)



A Mw6.3 in Xizang, Tibet, 2020 ascending S1 interferogram

arrows point to phase steps

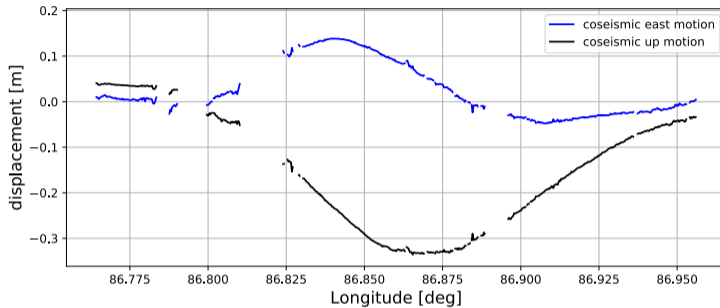


A Mw6.3 in Xizang, Tibet, 2020

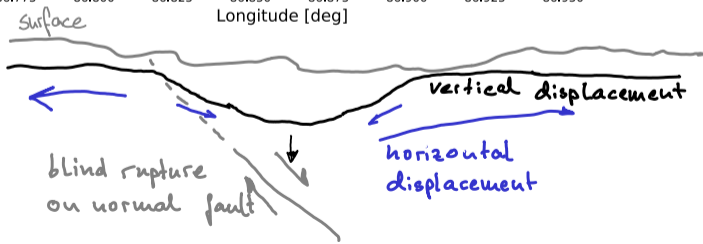
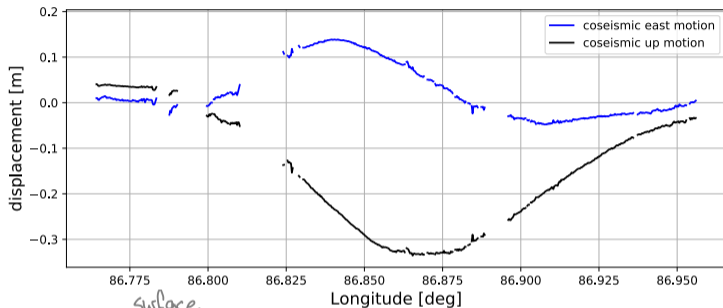
East component
of displacement

arrows point to phase steps

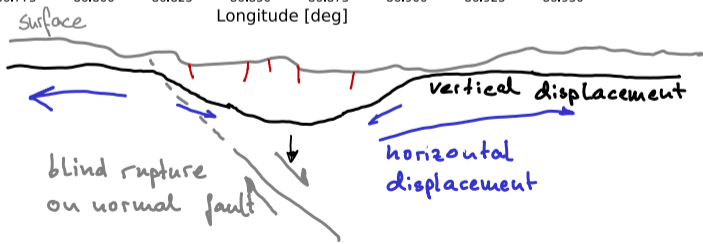
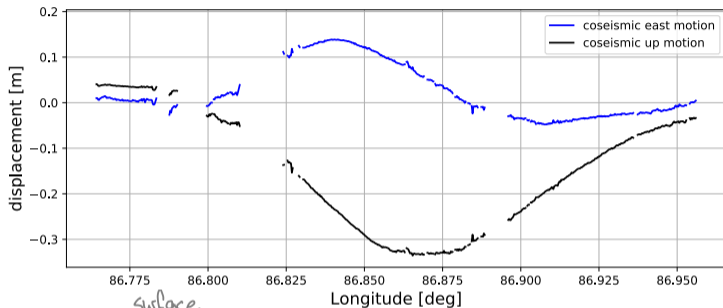
Quick change of perspective on the problem

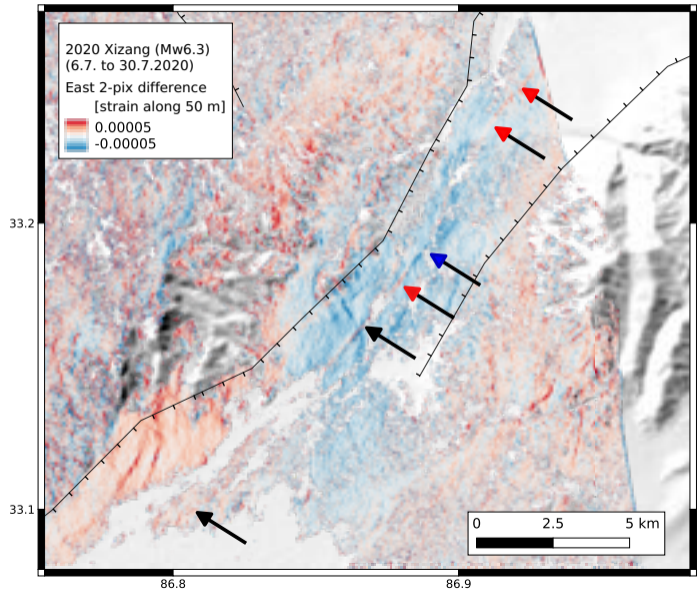


Quick change of perspective on the problem



Quick change of perspective on the problem





A Mw6.3 in Xizang, Tibet, 2020

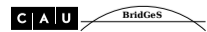
East component of displacement

available & shown components of strain vector:

$$\epsilon = \begin{pmatrix} \epsilon_{ee} & \epsilon_{en} \\ \epsilon_{ne} & \epsilon_{nn} \\ \epsilon_{(u+n)e} & \epsilon_{(u+n)n} \end{pmatrix}$$

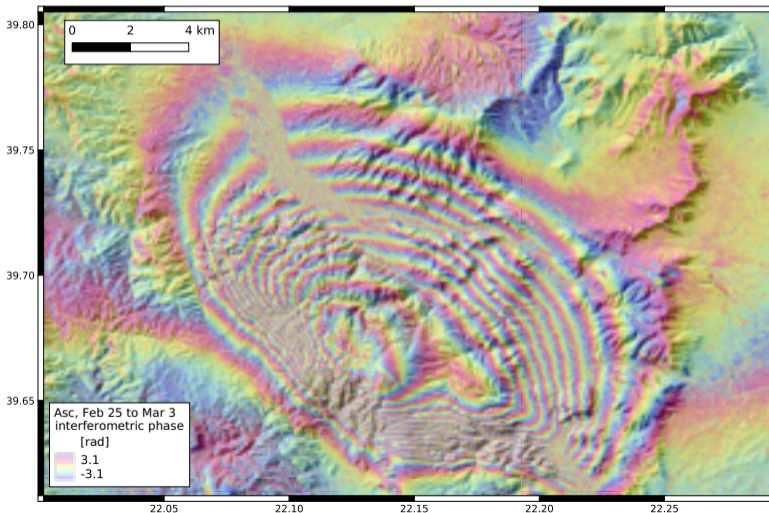
blue linear features:
east-side moves west

red linear features:
east-side moves east





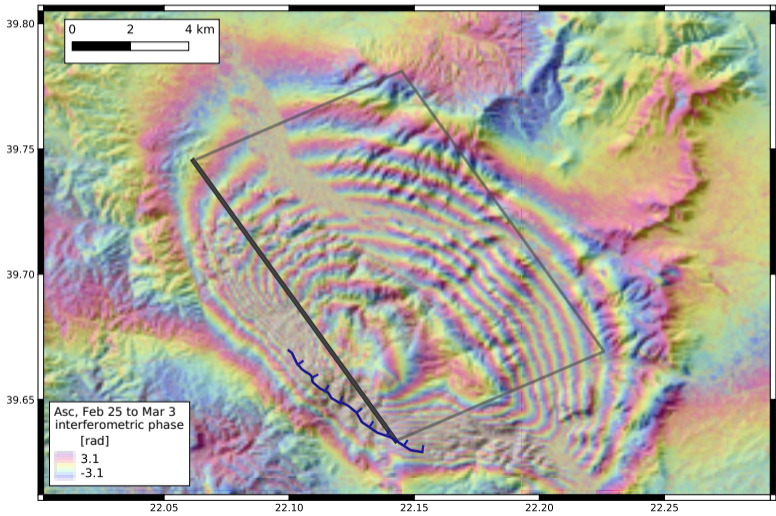
More fault activations with a M6.3 earthquake



Tyrnavos earthquake (Greece)
Mw6.3, on Mar 3 2020 (Greece)

Sentinel-1 interferogram
spanning 6 days

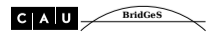
More fault activations with a M6.3 earthquake



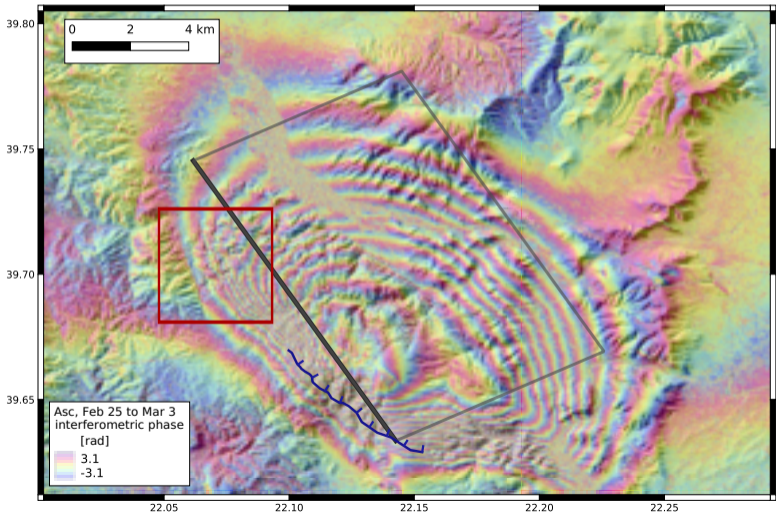
Tyrnavos earthquake
Mw6.3, on Mar 3 2020 (Greece)

Sentinel-1 interferogram
spanning 6 days

- coseism. surface rupture
- fault model projection



More fault activations with a M6.3 earthquake

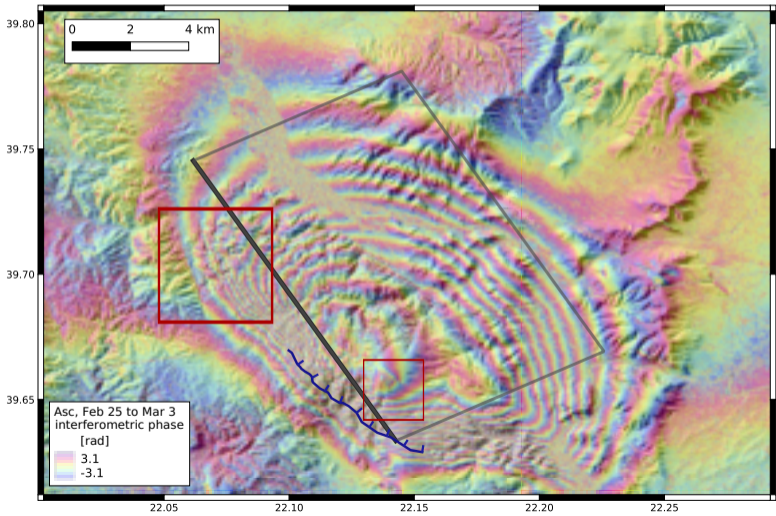


Tyrnavos earthquake
 M_w 6.3, on Mar 3 2020 (Greece)

Sentinel-1 interferogram
 spanning 6 days

- coseism. surface rupture
- fault model projection

More fault activations with a M6.3 earthquake

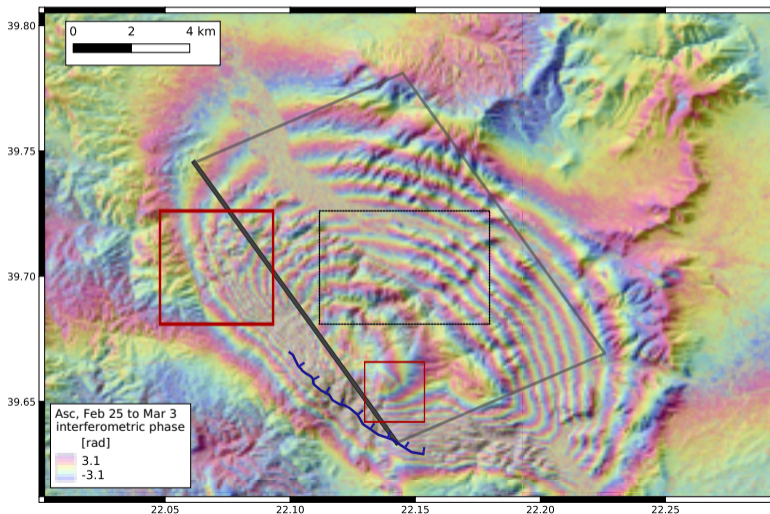


Tyrnavos earthquake
 M_w 6.3, on Mar 3 2020 (Greece)

Sentinel-1 interferogram
 spanning 6 days

- coseism. surface rupture
- fault model projection

More fault activations with a M6.3 earthquake



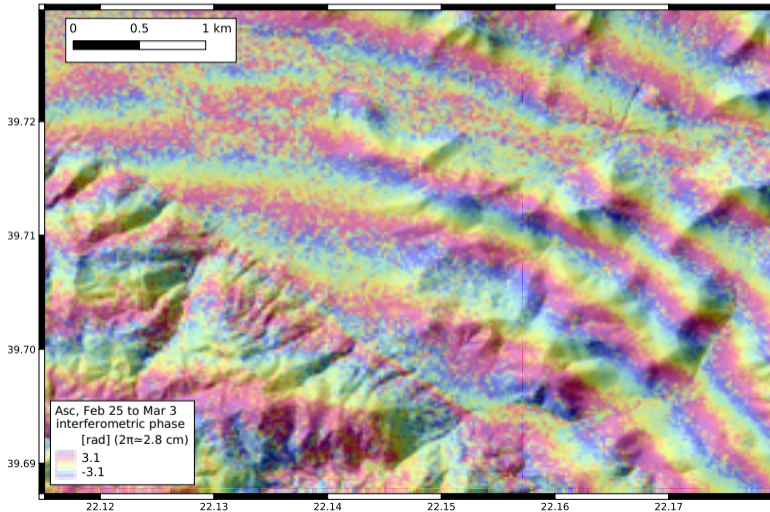
Tyrnavos earthquake
Mw6.3, on Mar 3 2020 (Greece)

Sentinel-1 interferogram
spanning 6 days

coseism. surface rupture

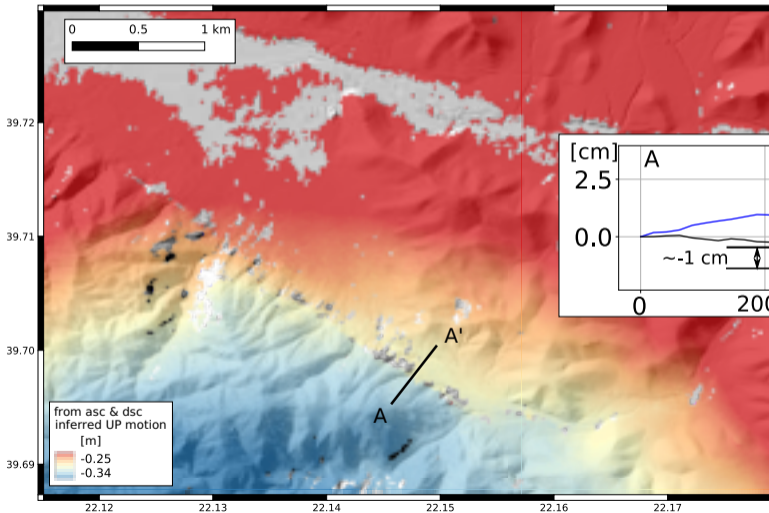
fault model projection

Observations of synseismic fault activation

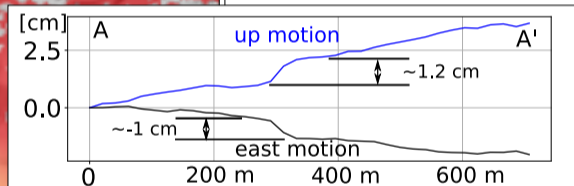


Observed character:
Phase jumps of ~ 1 cm, quite linear
and along kilometers at pre-existing faults.
Slip direction varies.

Observations of synseismic fault activation



Observed character:
Phase jumps of ~ 1 cm, quite linear
and along kilometers at pre-existing faults.
Slip direction varies.

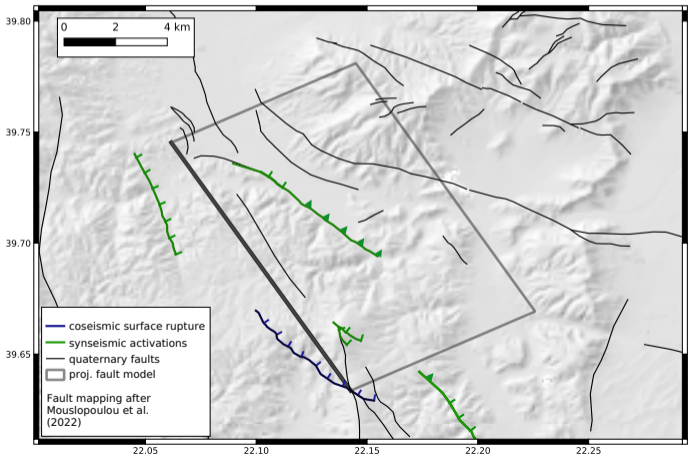


Here, the morphology reveals
a normal fault.
The displacements show a reverse
activation at the Vlachogianni fault.

Analysis of synseismic fault activation

Slip direction varies spatially. It sometimes flips along the same fault.

Mapping of synseismic fault activations



Normal and reverse faulting seems to prevail.

Any north components are only weakly projected in InSAR imagery and might be missed.

Is there a relationship of fault motion and coseismic stress change?

Analysing the surface strain field

based on displacement maps, here observed with InSAR

strain vector at surface:

$$\epsilon = \begin{pmatrix} \frac{\partial E}{\partial e} & \frac{\partial E}{\partial n} & \frac{\partial E}{\partial u} \\ \frac{\partial N}{\partial e} & \frac{\partial N}{\partial n} & \frac{\partial N}{\partial u} \\ \frac{\partial U}{\partial e} & \frac{\partial U}{\partial n} & \frac{\partial U}{\partial u} \end{pmatrix} = \begin{pmatrix} \epsilon_{ee} & \epsilon_{en} & \epsilon_{eu} \\ \epsilon_{ne} & \epsilon_{nn} & \epsilon_{nu} \\ \epsilon_{ue} & \epsilon_{un} & \epsilon_{uu} \end{pmatrix},$$

The **strain tensor** at the surface:

$$\epsilon = \begin{pmatrix} \epsilon_{ee} & \frac{1}{2}(\epsilon_{en} + \epsilon_{ne}) \\ \frac{1}{2}(\epsilon_{en} + \epsilon_{ne}) & \epsilon_{nn} \end{pmatrix},$$

with the *dilatation* being $\epsilon_{dil} = \epsilon_{ee} + \epsilon_{nn}$

Analysing the surface strain field

based on displacement maps, here observed with InSAR

strain vector at surface:

$$\epsilon = \begin{pmatrix} \frac{\partial E}{\partial e} & \frac{\partial E}{\partial n} & \frac{\partial E}{\partial u} \\ \frac{\partial N}{\partial e} & \frac{\partial N}{\partial n} & \frac{\partial N}{\partial u} \\ \frac{\partial U}{\partial e} & \frac{\partial U}{\partial n} & \frac{\partial U}{\partial u} \end{pmatrix} = \begin{pmatrix} \epsilon_{ee} & \epsilon_{en} & \epsilon_{eu} \\ \epsilon_{ne} & \epsilon_{nn} & \epsilon_{nu} \\ \epsilon_{ue} & \epsilon_{un} & \epsilon_{uu} \end{pmatrix},$$

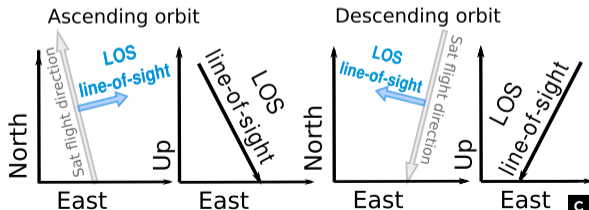
The **strain tensor** at the surface:

$$\epsilon = \begin{pmatrix} \epsilon_{ee} & \frac{1}{2}(\epsilon_{en} + \epsilon_{ne}) \\ \frac{1}{2}(\epsilon_{en} + \epsilon_{ne}) & \epsilon_{nn} \end{pmatrix},$$

with the *dilatation* being $\epsilon_{dil} = \epsilon_{ee} + \epsilon_{nn}$

Problem: strain vector from InSAR observations is incomplete and biased:

$$\epsilon = \begin{pmatrix} \epsilon_{ee} & \epsilon_{en} & \epsilon_{eu} \\ \epsilon_{ne} & \epsilon_{nn} & \epsilon_{nu} \\ \epsilon_{(u+n)e} & \epsilon_{(u+n)n} & \epsilon_{(u+n)u} \end{pmatrix}$$



Analysing the surface strain field

based on displacement maps, here observed with InSAR

strain vector at surface:

$$\epsilon = \begin{pmatrix} \frac{\partial E}{\partial e} & \frac{\partial E}{\partial n} & \frac{\partial E}{\partial u} \\ \frac{\partial N}{\partial e} & \frac{\partial N}{\partial n} & \frac{\partial N}{\partial u} \\ \frac{\partial U}{\partial e} & \frac{\partial U}{\partial n} & \frac{\partial U}{\partial u} \end{pmatrix} = \begin{pmatrix} \epsilon_{ee} & \epsilon_{en} & \epsilon_{eu} \\ \epsilon_{ne} & \epsilon_{nn} & \epsilon_{nu} \\ \epsilon_{ue} & \epsilon_{un} & \epsilon_{uu} \end{pmatrix},$$

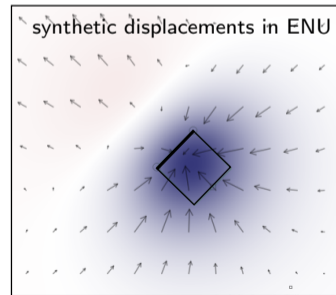
The **strain tensor** at the surface:

$$\epsilon = \begin{pmatrix} \epsilon_{ee} & \frac{1}{2}(\epsilon_{en} + \epsilon_{ne}) \\ \frac{1}{2}(\epsilon_{en} + \epsilon_{ne}) & \epsilon_{nn} \end{pmatrix},$$

with the *dilatation* being $\epsilon_{dil} = \epsilon_{ee} + \epsilon_{nn}$

Problem: strain vector from InSAR observations is incomplete and biased.

Work-around: Use a strain vector from synthetic displacements based on a seismic rupture model.



Analysing the surface strain field

based on displacement maps, here observed with InSAR

strain vector at surface:

$$\epsilon = \begin{pmatrix} \frac{\partial E}{\partial e} & \frac{\partial E}{\partial n} & \frac{\partial E}{\partial u} \\ \frac{\partial N}{\partial e} & \frac{\partial N}{\partial n} & \frac{\partial N}{\partial u} \\ \frac{\partial U}{\partial e} & \frac{\partial U}{\partial n} & \frac{\partial U}{\partial u} \end{pmatrix} = \begin{pmatrix} \epsilon_{ee} & \epsilon_{en} & \epsilon_{eu} \\ \epsilon_{ne} & \epsilon_{nn} & \epsilon_{nu} \\ \epsilon_{ue} & \epsilon_{un} & \epsilon_{uu} \end{pmatrix},$$

The **strain tensor** at the surface:

$$\epsilon = \begin{pmatrix} \epsilon_{ee} & \frac{1}{2}(\epsilon_{en} + \epsilon_{ne}) \\ \frac{1}{2}(\epsilon_{en} + \epsilon_{ne}) & \epsilon_{nn} \end{pmatrix},$$

with the *dilatation* being $\epsilon_{dil} = \epsilon_{ee} + \epsilon_{nn}$

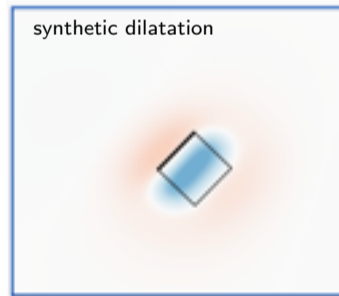
Problem: strain vector from InSAR observations is incomplete and biased.

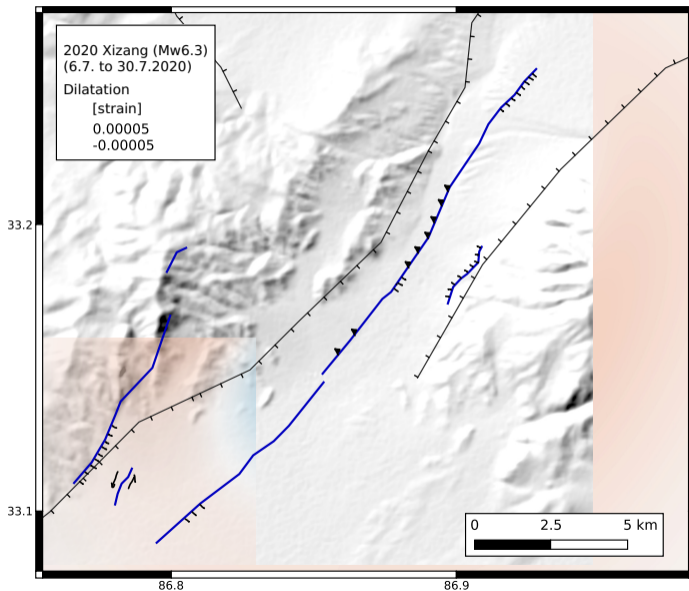
Work-around: Use a strain vector from synthetic displacements based on a seismic rupture model.

Reading dilatation:

A **positive** value shows a surface under **extension**.

A **negative** value shows a surface under **compression**.





A M_w 6.3 in Xizang, Tibet, 2020

predicted dilatation:

$$\epsilon = \begin{pmatrix} \epsilon_{ee} & \epsilon_{en} \\ \epsilon_{ne} & \epsilon_{nn} \\ \epsilon_{ue} & \epsilon_{un} \end{pmatrix}$$

Dilatation $\epsilon_{dil} = \epsilon_{ee} + \epsilon_{nn}$

red area: extension

blue area: compression

strain predictions based on
rupture modeling by
L. Diefenbacher

A Mw6.0 in Central Crete, 2021

predicted strain:

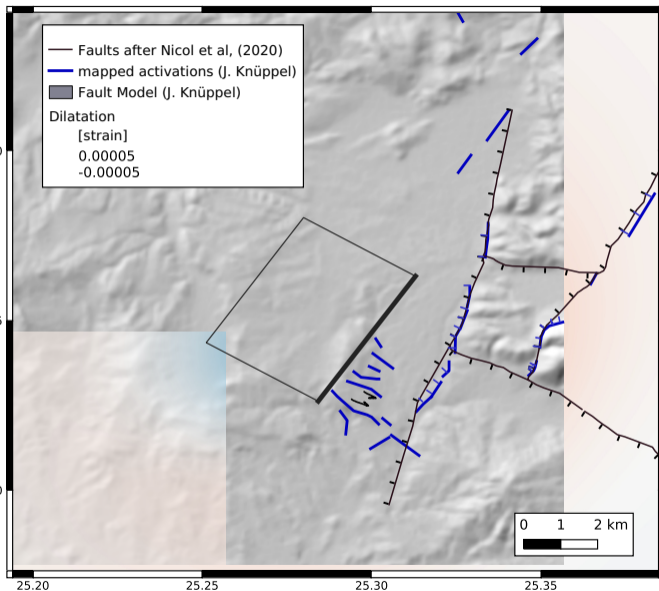
$$\epsilon = \begin{pmatrix} \epsilon_{ee} & \epsilon_{en} \\ \epsilon_{ne} & \epsilon_{nn} \\ \epsilon_{ue} & \epsilon_{un} \end{pmatrix}$$

Dilatation $\epsilon_{dil} = \epsilon_{ee} + \epsilon_{nn}$

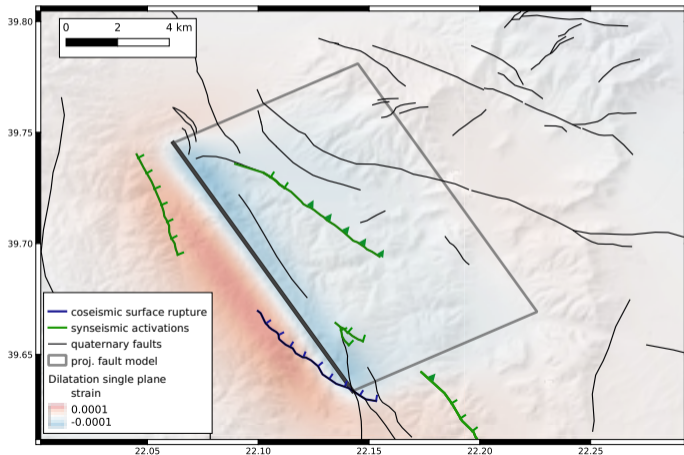
red area: extension

blue area: compression

strain predictions based on
rupture modeling by
J. Knüppel



Fault activation w.r.t. coseismic strain

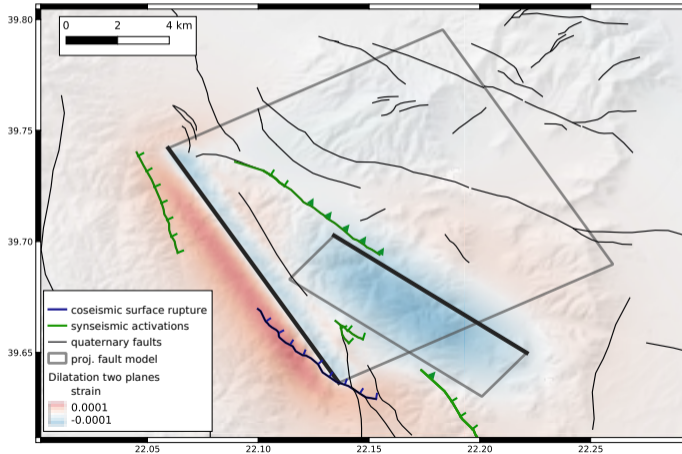


Normal and reverse faulting do not generally follow the strain regime pattern predicted by the simple fault model.

Deviation may stem from model simplifications:

- single rectangular fault with uniform slip
- horizontally layered medium

Fault activation w.r.t. coseismic strain

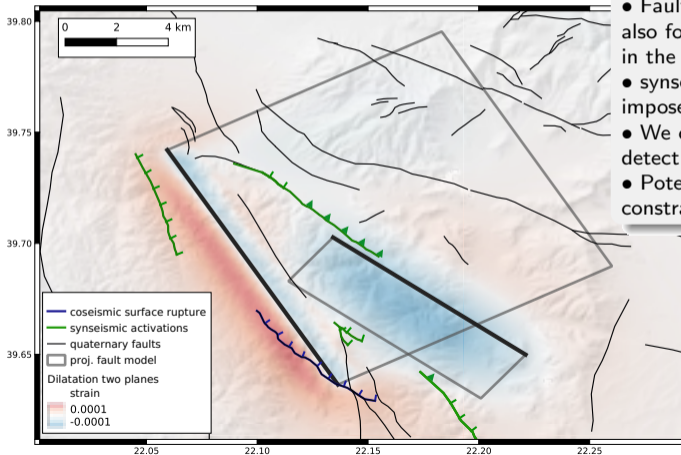


Normal and reverse faulting do not generally follow the strain regime pattern predicted by the simple fault model.

Deviation may stem from model simplifications:

- single rectangular fault with uniform slip
- horizontally layered medium
- More complex models can fit the observations better

Fault activation w.r.t. coseismic strain



Conclusions

- Faults react to earthquakes at neighbouring faults, also for earthquakes $M < 7$. (two more examples online in the supplementary talk material)
- synseismic fault activation releases part of the imposed coseismic stress.
- We can map very small fault slips from space and detect previously unmapped faults.
- Potentially these activation can help to better constrain models of the coseismic activation